Published in final edited form as:
Biomaterials. 2010 March ; 31(8): 2153–2162. doi:10.1016/j.biomaterials.2009.11.074.

The use of surface modified poly(glycerol-co-sebacic acid) in retinal transplantation

Christopher D. Pritchard[a,*], **Karin M. Arnér**[b], **Rebekah A. Neal**[c], **William L. Neeley**[a], **Peter Bojo**[a], **Erika Bachelder**[d], **Jessica Holz**[d], **Nicki Watson**[d], **Edward A. Botchwey**[c], **Robert S. Langer**[a], and **Fredrik K. Ghosh**[b]

[a] Department of Chemical Engineering, Massachusetts Institute of Technology, Cambridge, MA, 02139, USA

[b] Department of Ophthalmology, Lund University Hospital, Lund, SE-22185, Sweden

[c] Department of Biomedical Engineering, University of Virginia, Charlottesville, VA, 22908, USA

[d] W.M. Keck Microscopy Facility, Whitehead Institute, Cambridge, MA, 02142, USA

Abstract

Retinal transplantation experiments have advanced considerably during recent years, but remaining diseased photoreceptor cells in the host retina and inner retinal cells in the transplant physically obstruct the development of graft-host neuronal contacts which are required for vision. Recently, we developed methods for the isolation of donor photoreceptor layers *in vitro*, and the selective removal of host photoreceptors *in vivo* using biodegradable elastomeric membranes composed of poly(glycerolco-sebacic acid) (PGS). Here, we report the surface modification of PGS membranes to promote the attachment of photoreceptor layers, allowing the resulting composite to be handled surgically as a single entity. PGS membranes were chemically modified with peptides containing an arginine-glycine-aspartic acid (RGD) extracellular matrix ligand sequence. PGS membranes were also coated with electrospun nanofiber meshes, containing laminin and poly(epsilon-caprolactone) (PCL). Following *in vitro* co-culture of biomaterial membranes with isolated embryonic retinal tissue, composites were tested for surgical handling and examined with hematoxylin and eosin staining and immunohistochemical markers. Electrospun nanofibers composed of laminin and PCL promoted sufficient cell adhesion for simultaneous transplantation of isolated photoreceptor layers and PGS membranes. Composites developed large populations of recoverin and rhodopsin labeled photoreceptors. Furthermore, ganglion cells, rod bipolar cells and AII amacrine cells were absent in co-cultured retinas as observed by neurofilament, PKC and parvalbumin labeling respectively. These results facilitate retinal transplantation experiments in which a composite graft composed of a biodegradable membrane adhered to an immature retina dominated by photoreceptor cells may be delivered in a single surgery, with the possibility of improving graft-host neuronal connections.

Keywords

Cell adhesion; Elastomer; Laminin; Nanotopography; Polycaprolactone; Retina

[*] Corresponding author. Room E25-342, 45 Carleton St., Cambridge, MA, 02142, USA. Fax: +1 617 258 8827. cpritcha@mit.edu (C.D. Pritchard)..

1. Introduction

Retinal degenerative disease currently afflicts over 30 million patients worldwide [1]. This number is expected to increase in coming years, due not only to population growth but also the effect of aging populations, especially in developed countries. Age-related macular degeneration, hereditary retinal degeneration and retinal detachment involving the macula all lead to loss of photoreceptor function. The photoreceptor cells, located in the outer layer of the retina, are responsible for the transduction of light into electrical impulses. These signals are transmitted via neuronal connections through the inner retinal layers to the optic nerve and ultimately to the brain, resulting in a visual image. Therefore, retinal degenerative diseases lead to significant visual impairment and blindness.

When diseased photoreceptors are still present, but dysfunctional, current treatments may slow the progress of retinal degeneration [2,3]. At this stage of disease, gene therapy may also provide alleviation of symptoms [4]. However, there are currently no therapies that regenerate lost photoreceptors.

The prospect of retinal transplantation offers the possibility of replacing photoreceptors lost by degenerative disease. Experiments have been ongoing for more than two decades in a multitude of animal models, but to date, retinal transplantation is not available as a clinical treatment [5–7].

A critical issue remaining before clinical trials using retinal transplantation can be attempted is to increase the ability of graft and host retinal neurons to form functional connective neuronal networks. Graft-host neuronal connections have been shown to occur to some extent in rabbit models [8] but not in porcine models, which have a retinal vasculature that is more akin to the human eye [9]. In the porcine model, integration is hampered by the presence of two cell layers, namely remaining inner retinal cells in the transplant and diseased host photoreceptors [6]. In order to improve the probability of functional connection between host and graft retina, it is hypothesized that these two physical barriers must be removed.

A recent development, in this field of study, involves the removal of host photoreceptors by the insertion of a thin biodegradable elastomeric membrane between the retinal pigment epithelium and the outer nuclear layer [10]. The membrane, made from poly(glycerol-co-sebacic acid) (PGS) [11] disrupts blood supply from the choroid to the retina leading to selective removal of the photoreceptor layer. *In vivo*, the membrane degrades completely within 14 days, leaving a host retina composed of isolated inner retinal layers prepared to receive a complementary photoreceptor transplant.

In the current study, we aimed to combine the PGS membrane with donor retinal tissue, to create a composite graft that can be transplanted into the subretinal space in a single surgery. The creation of such a composite graft composed of a biodegradable membrane adhered to a retina dominated by photoreceptor cells may in future experiments enhance neuronal integration by providing close contact of grafted photoreceptors with host inner retinal cells. PGS membranes were chemically modified with peptides containing an arginine-glycine-aspartic acid (RGD) extracellular matrix ligand sequence [12]. Additionally, nanofiber meshes, composed of laminin, poly(epsilon-caprolactone) (PCL) or a blend of laminin and PCL, were electrospun onto PGS membranes.

The biomaterial membrane is intended ultimately to serve as a clinical paradigm that can be modified further to incorporate drugs or proteins with the aim of enhancing synaptic connections between grafts and the host nervous system. For example, neurotrophic factors such as brain derived neurotrophic factor (BDNF) or glial cell derived neurotrophic factor

(GDNF) have the ability to stimulate neuron growth [13] and may promote neurite sprouting from the transplant.

2. Materials and methods

All compounds and solvents were obtained from Sigma–Aldrich, St. Louis, MO, USA unless otherwise stated.

2.1. Preparation of poly(glycerol-co-sebacic acid) membranes

Poly(glycerol-co-sebacic acid) (PGS) branched polymer was prepared by poly-condensation as previously described [11]. Briefly, equimolar amounts (0.989 mol) of re-crystallized sebacic acid and anhydrous glycerol were charged to an oven-dried round bottom flask and reacted with stirring at 120 °C under argon. After 21 h, vacuum was applied and the mixture was reacted for another 64 h. The resulting material formed a white wax at room temperature.

Cross-linking of the PGS to an elastomer was carried out in a class 10,000 clean room. A 10:1 prepolymer:hardener mixture of poly(dimethylsiloxane) (PDMS) (Sylgard 184, Dow Corning, Midland, MI) was outgassed under vacuum and cured in a 10 cm Petri dish for 1 h at 60 °C. The resulting 10 cm diameter PDMS slab was plasma oxidized for 1 min to create a hydrophilic surface. The top surface was spin coated at 3000 rpm for 30 s with a 61.5 wt% aqueous sucrose solution (saturated at room temperature and 0.45 mm syringe filtered). The sucrose-coated PDMS was subsequently baked at 130 °C for 10 min and transferred to a hotplate at 120 °C. Molten PGS wax (120 °C) was poured onto the sucrose-coated PDMS slab, covering the entire surface, and subsequently cured at 120 °C under a 15 mtorr vacuum until the PGS lost any adhesiveness to a stainless steel spatula.

Subsequently, the mold was submerged in 18 MOhm water overnight and the PGS was peeled from the PDMS underwater. The resultant PGS disk was approximately 3 mm thick.

The PGS disk was cut into 5 × 5 × 3 mm blocks, embedded in Tissue-Tek OCT compound (Sakura, Torrance, CA) and rapidly frozen by immersion in ethanol cooled with dry ice. Frozen PGS was cryo-sectioned into 30 μm membranes at –30 °C with a Shur/Sharp Heavy Duty razor blade (TBS, Durham, NC). Thicker blades (0.5 mm or greater) and slow sectioning speeds were necessary to reduce vibration and warming of the blade from friction. Membrane thickness and uniformity was confirmed by scanning electron microscopy.

2.2. PGS – peptide coupling

2.2.1. Membrane activation—PGS samples (5 mm × 5 mm) were individually treated in a 0.1 w/v % solution of 1-(3-dimethylaminopropyl)-3-ethylcarbodiimide (EDC; 0.1 g) in 0.1 N 2-(*N*-morpholino)-ethanesulfonic acid (MES; 2.13 g) buffer in 18 MOhm water (100 mL, pH 3.5). Each sample was immersed in 1.5 mL of the EDC solution in 1.7 mL Eppendorf tubes at room temperature for 1 h, whilst shaking with a vortex mixer. The samples were washed in MES buffer (1 × 10 min; 1.5 mL/sample), and then in 18 MOhm water (2 × 10 min; 2 × 1.5 mL/sample). The activated PGS samples were directly used in the coupling reactions.

2.2.2. Membrane coupling to peptide GRGDS—The activated PGS sample (5 mm × 5 mm) was immersed into a 1 mM solution of the peptide sequence GRDGS (Anaspec, Freemont, CA) in phosphate buffered saline (PBS; pH 7.3) (1.5 mL) during 2 h at room

temperature, under shaking. The sample was rinsed 3 times for 10 min with 1 mL PBS and then with 1 mL 18 MOhm water for 10 min.

2.3. X-ray photoelectron spectroscopy analysis of peptide modified membranes

The surface chemical composition of the sample was determined by X-ray photoelectron spectroscopy (XPS) using a Surface Science Instruments SSX-100, equipped with a monochromatic aluminum X-ray source at 1486.8 eV. Charge neutralization was achieved using an electron flood gun. The vacuum in the analysis chamber was less than 2×10^{-9} torr during analysis. Photoelectrons were collected at an angle of 55° from the surface normal. A hemispherical analyzer was used with a pass energy of 150 eV for surveys and 50 eV for high-resolution scans. The peak areas were determined using Shirley background subtraction. The intensity ratios were converted into atomic concentration ratios using CasaXPS processing software (Casa Software Ltd., Cheshire, UK), which takes into account the instrument transmission function and provides a standard library of empirically-determined relative sensitivity factors.

2.4. Fabrication of electrospun nanofibers

Nanofibers consisting of poly(epsilon-caprolactone) (PCL) laminin and a blend of 10 wt% laminin in PCL of approximately 100 nm were electrospun onto 30 micron PGS sheets to create a bi-layer biomaterial membrane. Neuroretinal explants were subsequently cultured on a culture membrane with the outer layers facing downward and the PGS-nanofiber membranes on top, with the nanofiber side of the PGS sheet facing downward. Type 1 Laminin was isolated from murine Englebreth– Swarm–Holme tumor as previously described [14]. The laminin was provided as a gift by Stemgent, Inc. (Cambridge, MA). Electrospinning followed previously described protocols [15]. For laminin nanofibers, lyophilized laminin was dissolved in 1,1,1,3,3,3-hexafluoro-2-propanol (HFP) at 3 w/v% at 4 °C overnight. The solution was then mounted into an Aladdin syringe pump (World Precision Instruments, Sarasota, FL) using a disposable syringe and 18 gauge needle. PGS sheets mounted on glass cover slips were placed on the collector plate, and the laminin solution was dispensed at a flow rate of 1 mL/h and driving voltage of 15 kV across a 15 cm vertical gap onto the grounded copper collector, and hence onto the PGS sheets. Samples were dried completely and stored in dessicant at –20 °C. Laminin-PCL blend nanofibers were electrospun in a similar manner. A solution consisting of 10 wt% laminin and 90 wt% PCL with 8 w/v% total polymer dissolved in HFP was used as the initial solution. The same procedure as for laminin was used to electrospin the blend onto PGS sheets, though the driving voltage was increased to 20 kV to compensate for the higher viscosity of this solution. 18 wt% PCL was dissolved in 1:1 THF:DMF and electrospun at 20 kV in the same manner to fabricate PCL nanofibers.

2.5. Characterization of electrospun nanofibers

Samples were air dried for 24 h, mounted on aluminum stubs, and coated with a thin layer of carbon for scanning electron microscopy. A JSM-5910 General Purpose Scanning Electron Microscope(JEOL, Tokyo, Japan) was used to image the samples. To study the effect of hydration, samples were air dried after 5 days in culture medium. For scanning electron microscopy, samples were mounted on aluminum stubs and sputter coated with gold, and imaged using a JEOL 6400 Scanning Electron Microscope with Orion image processing (JEOL, Tokyo, Japan). Diameter measurements were made using the *measure* tool in Image J (NIH, Bethesda, MD), with at least 50 measurements per sample.

2.6. Culture procedure

2.6.1. Porcine tissue isolation—Eyes from Yorkshire/Hampshire pigs (gestational age of 114 days) were obtained from a local breeder (Lund, Sweden) and used for all experiments. Retinal tissue from E45 (45 days after conception) and E49-50 was used for culturing experiments, and E60 and E70 specimens were obtained as *in vivo* controls. The pregnant sow was euthanized by means of captive bolt and incision of the carotid arteries. The fetuses were collected by caesarean section and euthanized by decapitation. Both eyes were enucleated and immediately immersed in ice-cold CO_2-independent medium. The neuroretinas were carefully dissected free from the retinal pigment epithelium (RPE) and hyaloid vascular system with fine forceps. The optic nerve was thereafter cut with micro-scissors and neuroretinal pieces measuring approximately 4 × 4 mm were explanted on Millicell®-HA 0.45- μm culture plate inserts with the photoreceptor layer towards the membrane. All neuroretinas were put in culture within 240 min.

Explants were cultured in 1.2 mL Gibco D-MEM F12 medium –L-Glutamine (Gibco, Paisley, UK) supplemented with 10 vol% fetal calf serum. A cocktail containing 2 mM L-glutamine, 100 U/mL penicillin and 100 ng/mL streptomycin was added, and the retinas were maintained at 37 °C with 95% humidity and 5% CO_2.

2.6.2. Co-culture of retinal layers with biomaterial membranes—After two days, PCL-PGS and Laminin-PCL-PGS membranes measuring 2 × 3 mm were added to the explanted retinal specimens (12 each) while another 12 pieces were kept in culture without the addition of a membrane as *in vitro* controls. At this time half of the culture medium was exchanged, and this procedure was then repeated every second day. Specimens were kept under culture conditions for either 1 or 2 weeks (7–9 or 14–16 days).

All proceedings and treatment of animals were in accordance with the guidelines and requirements of the Government Committee on Animal Experimentation at Lund University and with the ARVO Statement for the Use of Animals in Ophthalmic and Vision Research.

2.7. Histology

For histologic examination, the explants were fixed for 1 h in 4% formalin, pH 7.3 in a 0.1 M Sørensen's phosphate buffer (PB). After fixation, the specimens were washed with 0.1 M Sørensen's PB, and then washed again using the same solution containing sucrose of rising concentrations (5–25%). They were then sectioned at 12 μm on a cryostat, and each 10th slide was stained with hematoxylin and eosin according to standard procedures.

For immunohistochemical staining, sections were incubated at room temperature with phosphate buffered saline (PBS) containing 0.25% Triton X-100 and 1% bovine serum albumin for 30 min. This was followed by incubation of the slides overnight with primary antibodies (Table 1). After incubation, the slides were rinsed in PBS and incubated with Texas-red-conjugated secondary antibodies (Jackson Immunoresearch, West Grove, PA, USA) for 50 min in room temperature and thereafter rinsed again and finally mounted in custom made Vectashield mounting media containing DAPI (4′,6-diaminidin-2-phenylindoldihydrochloride; Vector laboratories, California, USA).

For recoverin and vimentin double-labeling, the tissue was incubated with recoverin and vimentin antibodies for 18–20 h and rinsed in PBS-Triton. Subsequently, the tissue was incubated for 45 min in darkness with a mixture of the secondary antibodies conjugated with two fluorophores: anti-rabbit fluorescein isothiocyanate (FITC; Southern Biotechnology; Birmingham, AL, USA) and anti-mouse Texas red. The dilution of each secondary antibody was 1:200.

Neuroretinas derived from E60 and E70 eyes were used to compare cultured specimens with the corresponding *in vivo* counterparts. Sections from adult porcine retinas were used as positive controls. Negative controls were obtained by performing the complete labeling procedure without primary antibody on retinal sections from adult pigs. Photographs were obtained with a digital camera system (Olympus, Tokyo, Japan). Photographs were adjusted for brightness and contrast digitally.

3. Results

3.1. Membrane properties

3.1.1. PGS sheets—A variety of approaches for the fabrication of PGS membranes were attempted. A microtome was used with and without the PGS embedded in paraffin. The microtome was unable to cut PGS, and the material compressed at the point of contact with the microtome blade. Subsequently, a cryo-sectioning technique employed to fabricate PGS sheets was able to create 30 μm thick membranes (Fig. 1A). A slightly wavy surface was produced due to blade vibrations, as seen in the image by light and dark contours on the membrane surface. Compared to the edge of the membrane, which was cut by a standard laboratory razor blade, the cryo-sectioning technique created a smooth surface. To optimize the cryo-sectioning technique, the type of blade, temperature of the instrument, temperature of the frozen block, size of the frozen block and surface area of the PGS pieces were varied to identify conditions that would allow sectioning. After suitable parameters were obtained, we investigated how thin the PGS could be sectioned. A thickness of 30 μm was found to be the limit, as 20 μm sections were too fragile and readily folded upon themselves.

3.1.2. GRGDS peptide modification of PGS sheets—Analysis by XPS gave: C1s: 284.526 eV (98.56%); N1s: 399.335 eV (1.44%). Considering the theoretical monomer unit ((PGS)y + (PGS-GRGDS)x), i.e. ((C13H22O5)y + (C30H52N8O13)x), where $x + y = 1$, we calculated the atomic ratios as: $N/C = 8x/(30x + 13(1 – x))$ and $O/C = (13x + 5(1 – x))/(30x + 13(1 – x))$. From the experimental value (N/C = 0.0146), we found $x = 0.0245$, i.e. approximately 2.45% surface functionalization.

3.1.3. Characterization of electrospun nanofibers on PGS sheets—A thin-layered random network of PCL nanofibers was created on top of the PGS sheets (Fig. 1B). While some bead defects are visible, the overall morphology remains fibrous in structure. The laminin-PCL blended nanofibers created a denser network with fewer bead defects and visibly thicker fibers than PCL alone (Fig. 1D). Electrospinning of laminin alone also created a dense network with few defects, but markedly finer nanofibers than PCL and laminin-PCL blends (Fig. 1C). Table 2 reports the diameters of the three meshes. The mean diameters for dry nanofibers increased significantly with decreasing concentration of laminin from 65.38 nm for pure laminin to 101.50 nm for laminin-PCL blends to 175.12 nm for pure PCL. A one-way ANOVA showed significance for differences among groups ($p < 0.01$). Following hydration in culture medium, the mean diameter of the laminin-PCL blended nanofibers almost doubled to 199.21 nm, indicating that the networks are prone to swelling under aqueous conditions; however, the fibrous morphology of the mesh was retained (image not shown). Furthermore all of the networks possess a significant distribution of nanofiber size as evidenced by the standard deviations.

3.2. Surgical handling results

Table 3 shows the results of mechanical integrity of the co-cultured membranes during loading/unloading into the transplantation instrument for a variety of biomaterial membranes and retinas. The PGS membranes without chemical or physical modifications cultured for 7–

14 days with E40 porcine retinas demonstrated insufficient adherence between the biomaterial and retina during transplantation.

By contrast, the RGD peptide modified membranes (RGD-PGS), as well as the PGS membrane coated with pure laminin nanofibers (Laminin-PGS), demonstrated improved adherence over PGS. However, the membrane and retina dissociated after the composite was pushed out of the transplantation device, rendering the RGD PGS and Laminin-PGS membranes unsuitable for *in vivo* transplantation in pig models.

Two of the nanofiber mesh coated PGS membranes (PCL-PGS and Laminin-PCL-PGS) seemed to integrate quite well with the porcine retinas. It was possible to dissect these composites from the culture membrane, place them in the transplantation device, and eject them without the two components dissociating.

3.3. Histology and immunohistochemistry

Histological sections showed that some porcine retinal explants were double folded, whether or not they were co-cultured with biomaterial membranes. This was probably due to the fact that some of the vitreous membrane remained in place during isolation of the retinal layer. The vitreous membrane should ideally be completely removed prior to transplantation. PGS membranes co-cultured for 7–14 days with E40 porcine retinas developed photo-receptors (images not shown). The cells in the retinas co-cultured with PGS were somewhat less organized than *in vitro* controls (images not shown). However, the controls were more folded, indicating that the addition of PGS membranes flattened the retinal cultures. In retinas co-cultured with RGD-PGS sheets, processes extending from retinal cultures towards the RGD-PGS sheets were observed in some sections (images not shown).

Neurofilament staining in retinas co-cultured *in vitro* with PCLPGS or Laminin-PCL-PGS membranes for 9 or 16 days demonstrated an absence of ganglion cells in these retinas (Fig. 2A–D). Neurofilament labeling was evident in the ganglion cell layer for E49 *in vitro* controls cultured for 7 days (Fig. 2E), but eventually disappeared from the nerve fiber layer (NFL) after 14 days (Fig. 2F). By comparison, neurofilament positive axons were intensely labeled in the NFL of *in vivo* controls (Fig. 2G, H).

PKC labeled rod bipolar cells and parvalbumin labeled AII amacrine cells were not evident in retinas co-cultured with biomaterial membranes or in *in vitro* controls (Fig. 3A–F). Tube-like structures appeared as rosettes in some sections (indicated by arrows in Fig. 3B, C). In E70 *in vivo* controls, PKC labeled rod bipolar cells were visible in the inner nuclear layer (INL) and ganglion cell layer (GCL). Neurites were intensely labeled with PKC in the inner plexiform layer (IPL) (Fig. 3G). Parvalbumin labeled amacrine cells were present in the GCL (Fig. 3H).

Large populations of recoverin labeled photoreceptors were present in all retinas co-cultured with biomaterial membranes (Fig. 4A–D). Recoverin labeled photoreceptors were located predominately in the outer retinal layers of *in vitro* controls (Fig. 4E, F), and in the outer nuclear layer (ONL) of *in vivo* controls (Fig.4G, H).

Vimentin labeled Müller cells were well organized in retinas co-cultured with biomaterial membranes, with processes apparently extending into the nanofiber networks (Fig. 4A–D). Vertically arranged vimentin labeled fibers were present in inner retinal layers of *in vitro* and *in vivo* controls (Fig. 4E–H). The retinas co-cultured with membranes did not express vimentin at the same intensity as the controls.

Rhodopsin labeling revealed an abundance of rod photoreceptors in outer nuclear layer (ONL) of retinas co-cultures with biomaterial membranes (Fig. 5A–D). Rhodopsin labeled rods were also present in *in vitro* and *in vivo* controls (Fig. 5E–H).

4. Discussion

In a previous study, 45 μm thick membranes were implanted into the subretinal space of rabbits, with one case of mechanical noncompliance resulting in damage to the RPE and choroid [10]. In this study, we were able to fabricate 30 μm membranes using a cryo-sectioning technique. By making the membranes thinner, they also became more flexible. Therefore mechanical disruption of the retina during and following implantation, as well as subretinal gliosis, may be reduced by using 30 μm membranes. PGS membranes without modification did not adhere firmly to the cultured retinas. However, the controls were more folded, indicating that the addition of PGS membranes flattened the retinal cultures. This is considered desirable, as it may help preserve the laminated morphology of the photoreceptor layer following transplantation.

A nanofiber architecture was necessary to provide sufficient attachment of porcine retinal layers for surgical handling and transplantation. Nanofibers have been demonstrated to be effective at providing a bridge within peripheral nerve tubes for axonal regeneration both *in vitro* and *in vivo* [16–18]. Polymeric nanofibers have also exhibited nerve guidance capabilities in the central nervous system. Structure and geometry have been shown to play very significant roles in cell adhesion and guidance. For example, smaller diameter nanofibers appear to yield longer and faster outgrowth of neurites than larger diameter nanofibers [19]. The paper also reports significantly longer outgrowth of neurites occurred on laminin coated fibers compared to fibronectin fibers with fibers of the same diameter. In another study, collagen-functionalized nanofibers improved cell adhesion and migration compared to non-functionalized nanofibers [20]. The authors suggested that functionalizing nanofibers with fibronectin or laminin may potentially have a greater effect than collagen by stimulating integrin binding through peptide sequences such as RGD, IKVAV and YISGR. The addition of laminin to the nanofibers coating the PGS sheets was to promote neurite in-growth into the membrane and to facilitate neuronal connection between graft and host following degradation of the biomaterial by orienting graft neurites towards host inner nuclear layers. However, no evidence of neurite in-growth into the nanofiber mesh was observed *in vitro* in this study. Furthermore, based on the antibodies tested in this study, no differences were detected between membranes with PCL nanofibers and membranes with PCL and laminin blended fibers. The structural arrangement and bioactivity of the laminin following electrospinning warrants further investigation.

In some histological sections of retinas co-cultured with nanofiber coated membranes, it appeared as though some tissue elements have penetrated the fiber network showing promising in-growth (images not shown). These processes label for vimentin and are thus at least partly of Müller origin. Comparing retinas co-cultured with membranes to *in vitro* controls it was observed that the retinas with membranes do not express vimentin in Müller cells at the same intensity as controls. Low vimentin expression in Müller cells is difficult to interpret. The cells display a normal structure, but the membrane may influence nutrition.

Persisting inner nuclear cells in the donor tissue are thought to inhibit integration of donor photoreceptors with the host inner nuclear layers. Therefore, the removal of these cells prior to transplantation may be favourable for neuronal connection of the co-cultured retinal layer upon degradation of the biomaterial. Neurofilament remains for some time in E49 *in vitro* controls cultured for 7 days (E49-7DIV), but not in the PCL-PGS or Laminin-PCL-PGS cultured specimens. This removal of ganglion cells may be due to retrograde degeneration as

the optic nerve is cut, enhanced by the ischemia induced by the sectioning of retinal vessels as well as placing the biomaterial membranes on top of the retinal layers *in vitro*. Even in E60 *in vivo* controls, PKC (rod bipolars) and parvalbumin (amacrine cells) are not abundant, indicating that retinal tissue isolated prior to 60 days post-embryogenesis is ideal for transplantation.

In a prior study, the 45 μm PGS membranes degraded within 28 days in the subretinal space in rabbits [10]. This duration was sufficiently long enough for the selective removal of host photo-receptors in rabbit eyes. Whilst the 30 μm PGS membranes will degrade more rapidly, PCL is likely to degrade over a longer period of time *in vivo* than PGS. Therefore, the nanofibers may persist for longer than the PGS membrane. This may or may not be advantageous. Pig photoreceptors are likely to be more resilient to ischemic trauma than rabbits, and may require a longer separation time from the retinal pigment epithelium (RPE). On the other hand, a prolonged separation between donor photoreceptors and the host inner nuclear layer (INL) may lead to undesired subretinal gliosis.

5. Conclusion

We have shown that electrospun nanofibers composed of laminin and PCL promoted sufficient cell adhesion for simultaneous transplantation of isolated photoreceptor layers and PGS membranes. Composites developed large populations of recoverin and rhodopsin labeled photoreceptors. Furthermore, ganglion cells, rod bipolar cells and AII amacrine cells were absent in co-cultured retinas as observed by neurofilament, PKC and parvalbumin labeling respectively. It may now be possible to conduct retinal transplantation experiments in which a composite graft composed of a biodegradable membrane adhered to an immature retina dominated by photoreceptor cells are delivered in a single surgery. By selective removal of host photoreceptors and delivery of a photoreceptor transplant without inner retinal cells, this approach may improve graft-host neuronal connections.

Acknowledgments

We thank Kurt Broderick for assistance with clean room operation (MTL, MIT, Cambridge, MA), Dr. Anthony Garratt-Reed and Libby Shaw for assistance with SEM and XPS (CMSE, MIT, Cambridge, MA), Jonathan Shu for assistance with XPS (Cornell, NY), the staff of the Edgerton Center Student Shop for assistance with building the electrospinning apparatus (MIT, Cambridge, MA), and Kerry Mahon for providing lab space and materials for electro-spinning (Stemgent, Inc., Cambridge, MA). We thank Elizabeth Pritchard for writing assistance (Starnberg, Germany). This work was supported by The Faculty of Medicine, University of Lund, The Swedish Research Council, The Princess Margaretas Foundation for Blind Children, the Torsten and Ragnar Söderberg Foundation, the National Institutes of Health (Grants DE013023 and HL060435), and the Richard and Gail Siegal Gift Fund. C.D.P. was supported by the MIT/CIMIT Medical Engineering Fellowship. C.D.P. and P.B. were supported by a gift to MIT by In Vivo Therapeutics Corporation. W.L.N. was supported by the NIH under Ruth L. Kirschstein National Research Service Award 1 F32 EY018285-01 from the National Eye Institute.

Appendix

Figures with essential colour discrimination. Figs. 2–5 in this article may be difficult to interpret in black and white. The full colour images can be found in the on-line version, at doi:10.1016/j.biomaterials.2009.11.074.

References

1. Ambati J, Ambati BK, Yoo SH, Ianchulev S, Adamis AP. Age-related macular degeneration: etiology, pathogenesis, and therapeutic strategies. Surv Ophthalmol. 2003; 48:257–93. [PubMed: 12745003]

2. Berson EL, Rosner B, Sandberg MA, Weigel-DiFranco C, Moser A, Brockhurst RJ, et al. Further evaluation of docosahexaenoic acid in patients with retinitis pigmentosa receiving vitamin A treatment: subgroup analyses. Arch Ophthalmol. 2004; 122:1306–14. [PubMed: 15364709]

3. Berson EL, Rosner B, Sandberg MA, Hayes KC, Nicholson BW, Weigel-DiFranco C, et al. A randomized trial of vitamin A and vitamin E supplementation for retinitis pigmentosa. Arch Ophthalmol. 1993; 111:761–72. [PubMed: 8512476]

4. Acland GM, Aguirre GD, Bennett J, Aleman TS, Cideciyan AV, Bennicelli J, et al. Long-term restoration of rod and cone vision by single dose rAAV-mediated gene transfer to the retina in a canine model of childhood blindness. Mol Ther. 2005; 12:1072–82. [PubMed: 16226919]

5. Turner JE, Blair JR. Newborn rat retinal cells transplanted into a retinal lesion site in adult host eyes. Brain Res. 1986; 391:91–104. [PubMed: 3955383]

6. Ghosh F, Wong F, Johansson K, Bruun A, Petters RM. Transplantation of full-thickness retina in the rhodopsin transgenic pig. Retina. 2004; 24:98–109. [PubMed: 15076950]

7. Maclaren RE, Pearson RA, Macneil A, Douglas RH, Salt TE, Akimoto M, et al. Retinal repair by transplantation of photoreceptor precursors. Nature. 2006; 444:203–7. [PubMed: 17093405]

8. Ghosh F, Bruun A, Ehinger B. Graft-host connections in long-term full thickness embryonic rabbit retinal transplants. Invest Ophthalmol Vis Sci. 1999; 40:126–32. [PubMed: 9888435]

9. Prince, JH.; Diesem, DC.; Eglitis, I.; Ruskell, GL. The pig anatomy and histology of the eye and orbit in domestic animals. Charles C Thomas; Springfield: 1960. p. 210-233.

10. Ghosh F, Neeley WL, Arnér K, Langer RS. Tissue Engineering Part A. in press. doi:10.1089/ten.tea.2008.0450.

11. Wang Y, Ameer GA, Sheppard BJ, Langer RS. A tough biodegradable elastomer. Nat Biotechnol. 2002; 20:602–6. [PubMed: 12042865]

12. Hersel U, Dahmen C, Kessler H. RGD modified polymers: biomaterials for stimulated cell adhesion and beyond. Biomaterials. 2003; 24:4385–415. [PubMed: 12922151]

13. Thanos C, Emerich D. Delivery of neurotrophic factors and therapeutic proteins for retinal diseases. Expert Opin Biol Ther. 2005; 5:1443–52. [PubMed: 16255648]

14. Kleinman HK, McGarvey ML, Liotta LA, Robey PG, Tryggvason K, Martin GR. Isolation and characterization of type IV procollagen, laminin and heparin sulfate proteoglycan from the EHS sarcoma. Biochemistry. 1982; 21:6188–93. [PubMed: 6217835]

15. Neal RA, McClugage SG, Link MC, Sefcik LS, Ogle RC, Botchwey EA. Laminin nanofiber meshes that mimic morphological properties and bioactivity of basement membranes. Tissue Eng Part C Methods. 2009; 15:11–21. [PubMed: 18844601]

16. Corey JM, Lin DY, Mycek KB, Chen Q, Samuel S, Feldman EL, et al. Aligned electrospun nanofibers specify the direction of dorsal root ganglia neurite growth. J Biomed Mater Res A. 2007; 83:636–45. [PubMed: 17508416]

17. Kim YT, Haftel VK, Kumar S, Bellamkonda RV. The role of aligned polymer fiber-based constructs in the bridging of long peripheral nerve gaps. Biomaterials. 2008; 29:3117–27. [PubMed: 18448163]

18. Clements IP, Kim YT, English AW, Lu X, Chung A, Bellamkonda RV. Thin-film enhanced nerve guidance channels for peripheral nerve repair. Biomaterials. 2009; 30:3834–46. [PubMed: 19446873]

19. Wen X, Tresco PA. Effect of filament diameter and extracellular matrix molecule precoating on neurite outgrowth and Schwann cell behavior on multifilament entubulation bridging device in vitro. J Biomed Mater Res A. 2006; 76:626–37. [PubMed: 16287096]

20. Gerardo-Nava J, Führmann T, Klinkhammer K, Seiler N, Mey J, Klee D, et al. Human neural cell interactions with orientated electrospun nanofibers in vitro. Nanomed. 2009; 1:11–30.

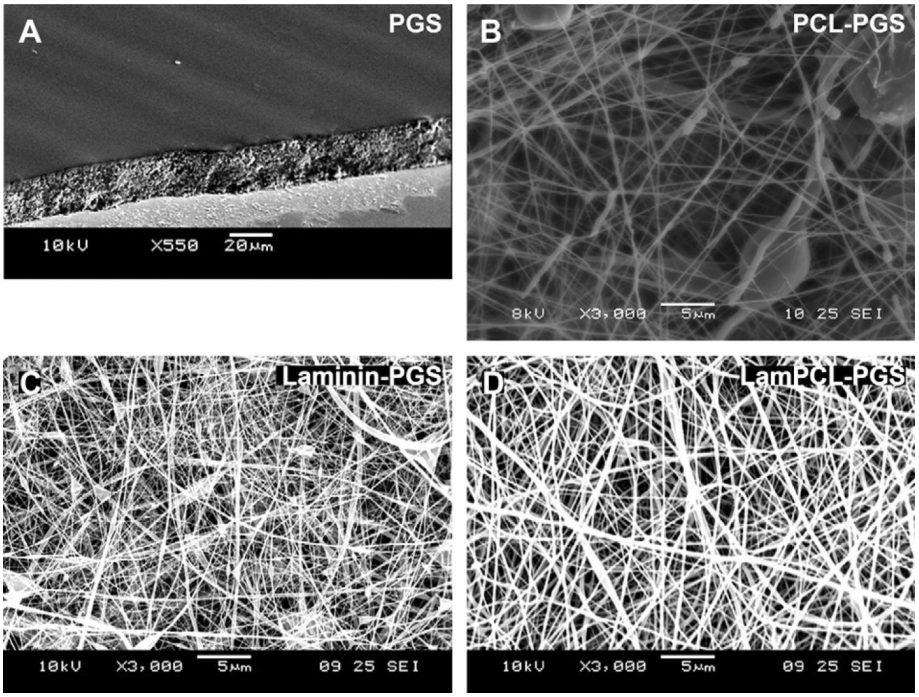

Fig. 1.

Scanning electron microscope images of membranes. A: 30 μm PGS sheet. Edge view at 60°. B–D: Nanofibers electrospun onto PGS sheets (B: PCL, C: Laminin, D: Laminin-PCL nanofibers). Top view.

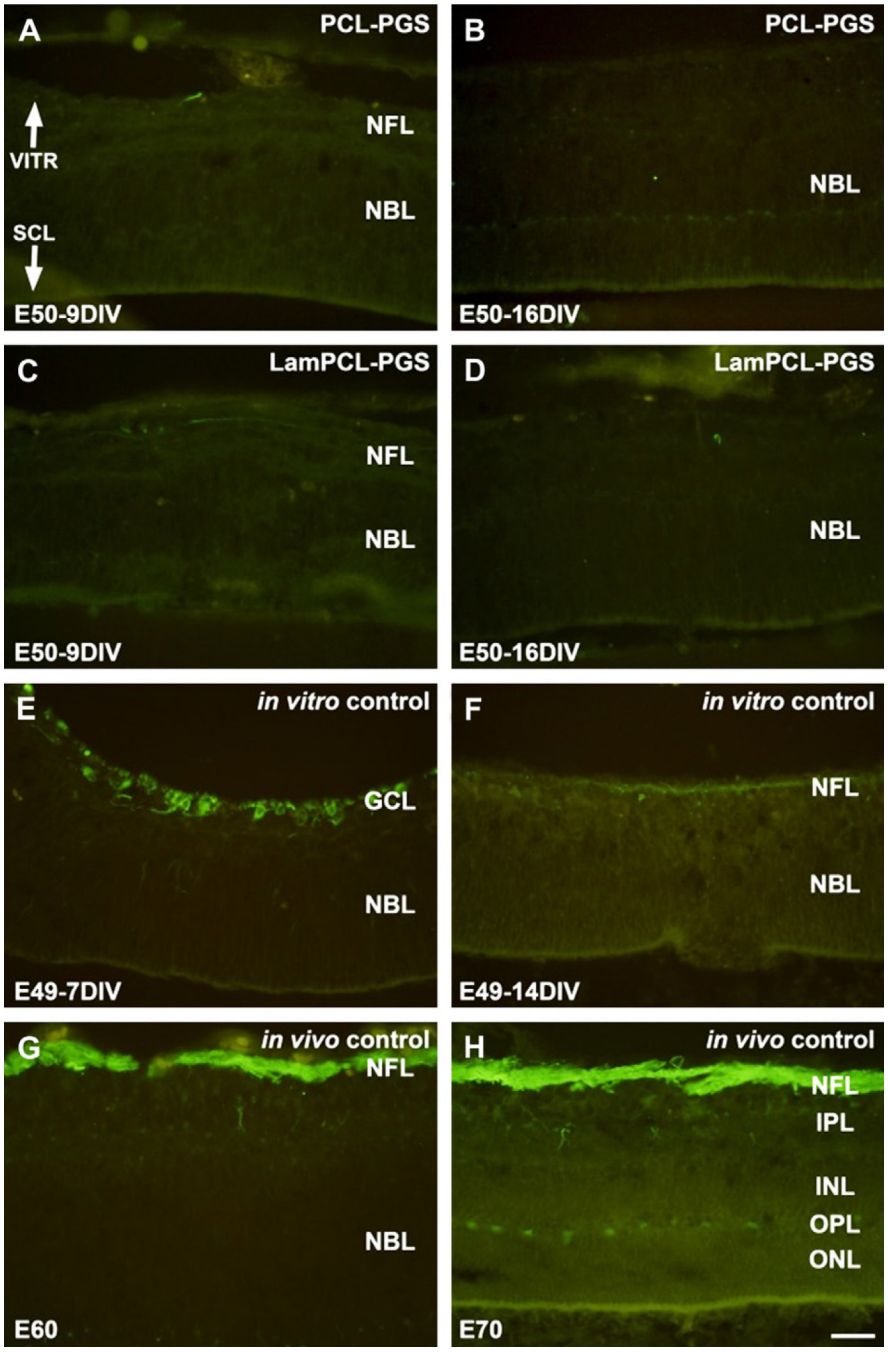

Fig. 2.

Neurofilament staining of fetal porcine retina. A–D: E50 retinas co-cultured for 9 (A, C) and 16 (B, D) days *in vitro* with PGS membranes coated with PCL (A, B) or laminin-PCL blend (C, D) nanofibers. Neurofilament staining is absent in the retinas co-cultured with nanofiber coated PGS membranes. E–F: E49 retinas cultured for 7 (E) and 14 (F) days *in vitro*. Neurofilament positive ganglion cells are visible in the ganglion cell layer (E). However, neurofilament staining is less evident following longer culture *in vitro* (F). G–H: E60 (G) and E70 (H) *in vivo* retina specimens. Neurofilament positive axons are visible in the nerve fiber layer (G). Intensely labeled neurofilament positive axons in the nerve fiber layer are visible, and horizontal cells in the outer part of the INL are also labeled (H). Neurofilament

staining is less pronounced in *in vitro* specimens (E–F) compared to *in vivo* specimens (G–H). VITR, vitreal (inner) aspect, SCL, sclera (outer) aspect. Scale bar = 50 microns.

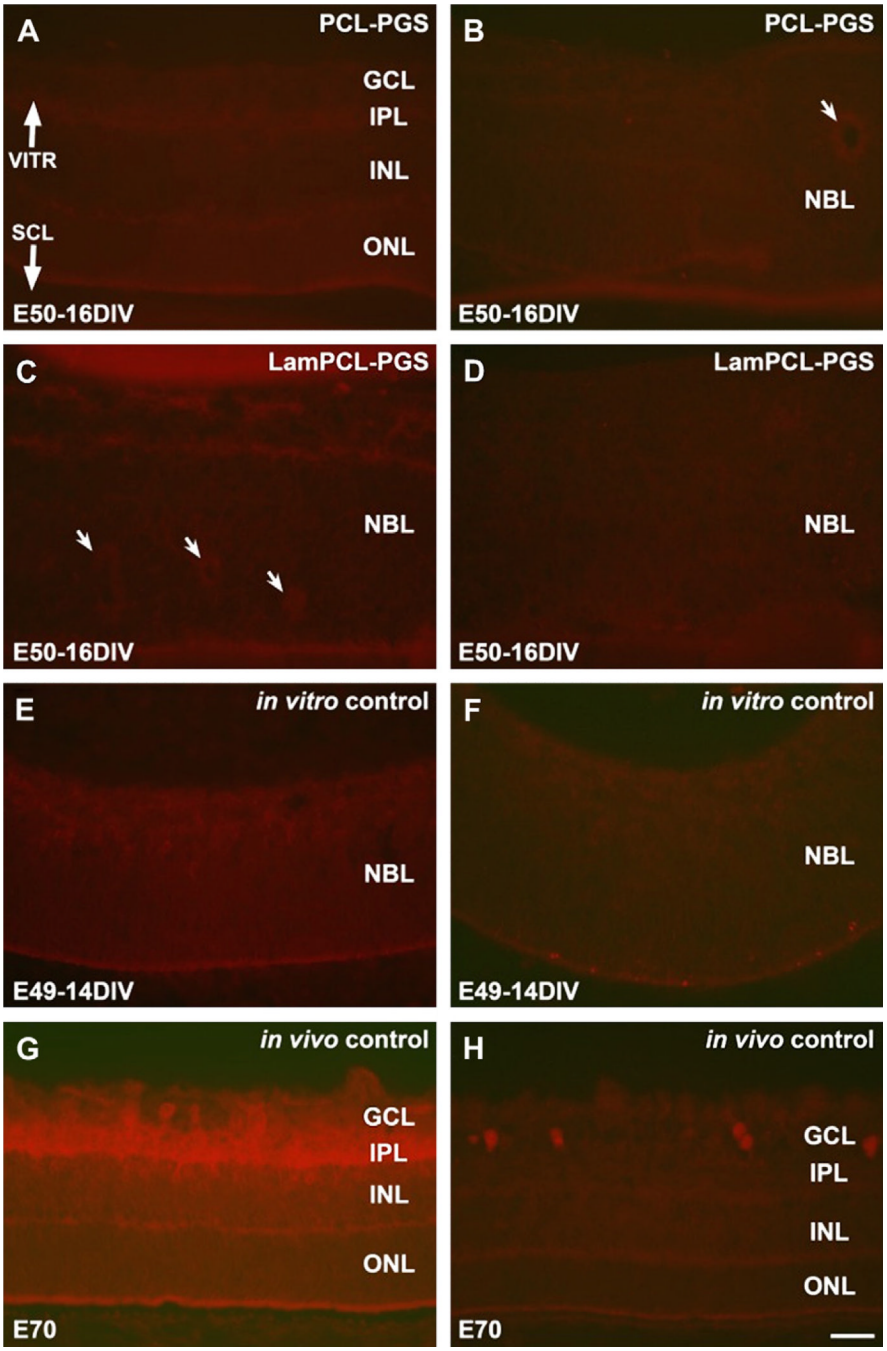

Fig. 3.

PKC (left column) and parvalbumin (right column) staining of fetal porcine retina. A–D: E50 retinas co-cultured for 16 days *in vitro* with PGS membranes coated with PCL (A, B) or laminin-PCL blend (C, D) nanofibers. Rosettes (arrows) are present in some sections (B, C). E–F: E49 retinas cultured for 14 days *in vitro*. PKC labeled rod bipolar cells and parvalbumin labeled amacrine cells are not abundant in any retinas cultured *in vitro* (A–F). G–H: E70 *in vivo* retina specimens. PKC labeled rod bipolar cells are seen in the inner part of the INL and in the GCL with intense labeling of neurites in the IPL (G). Parvalbumin labeled amacrine cell bodies are found in the GCL (H). VITR, vitreal (inner) aspect, SCL, sclera (outer) aspect. Scale bar = 50 microns.

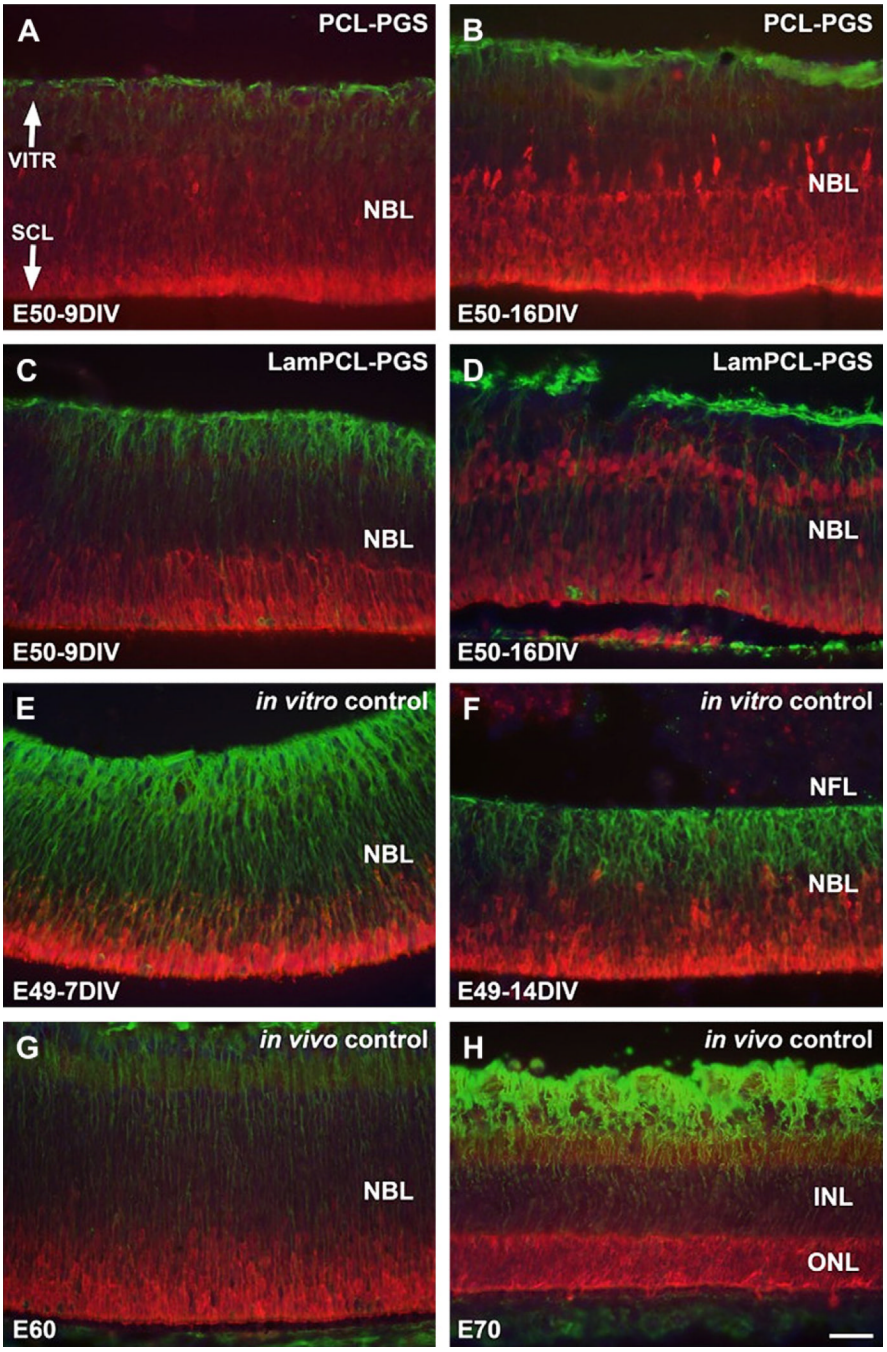

Fig. 4.

Recoverin (red) and vimentin (green) double-labeling of fetal porcine retina. A–D: E50 retinas co-cultured for 9 (A, C) and 16 (B, D) days *in vitro* with PGS membranes coated with PCL (A, B) or laminin-PCL blend (C, D) nanofibers. Müller cells are well organized, large populations of recoverin labeled photoreceptors are visible, and vimentin labeled processes extend into the nanofiber network. E–F: E49 retinas cultured for 7 (E) and 14 (F) days *in vitro*. Recoverin labeled photoreceptors are found mainly in outer retinal layers, and vertically arranged vimentin labeled fibers are visible with strong intensity corresponding to inner retinal layers. G–H: E60 (G) and E70 (H) *in vivo* retina specimens. Recoverin labeled photoreceptors are visible with highest intensity in the outer retinal layers, and vertically

arranged vimentin labeled fibers are visible (G). Recoverin labeled photoreceptor cells are seen in the entire ONL, and Müller cell processes display vimentin labeling throughout the retina with strong intensity corresponding to the inner retinal layers (H). Vimentin labeling of Müller cells is less intense in retinas co-cultured with PGS-nanofiber membranes (A–D) compared to controls (E–H). VITR, vitreal (inner) aspect, SCL, sclera (outer) aspect. Scale bar = 50 microns.

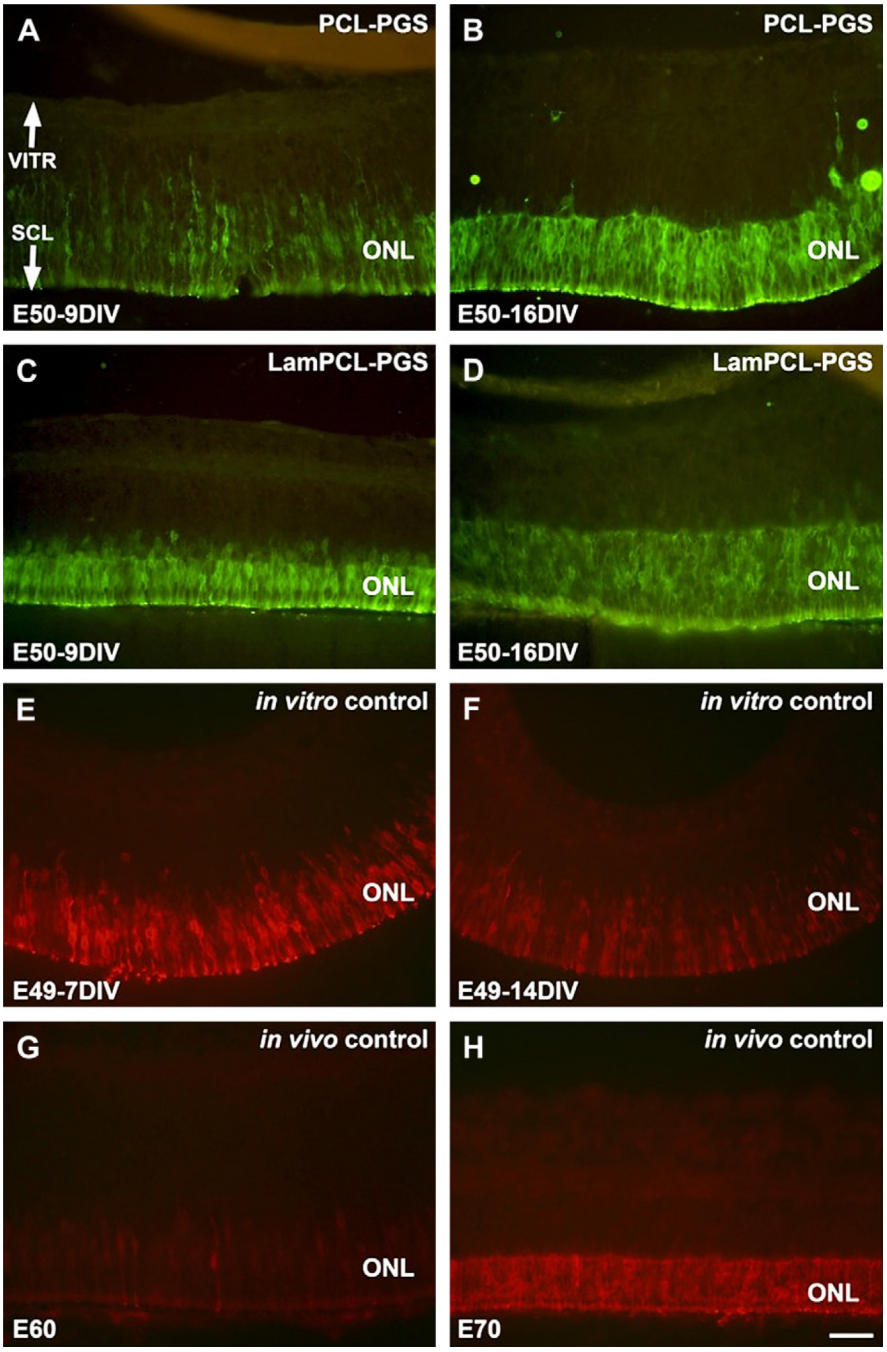

Fig. 5.

Rhodopsin staining of fetal porcine retina. A–D: E50 retinas co-cultured for 9 (A, C) and 16 (B, D) days *in vitro* with PGS membranes coated with PCL (A, B) or laminin-PCL blend (C, D) nanofibers. Rhodopsin labeled rod photoreceptors are visible in the outer nuclear layers of retinas, and survive at least 16 days in co-culture with PGS-nanofiber membranes. E–F: E49 retinas cultured for 7 (E) and 14 (F) days *in vitro*. Rhodopsin labeled rod photoreceptors are visible in the outer nuclear layer. G–H: E60 (G) and E70 (H) *in vivo* retina specimens. Rhodopsin labeled rod photoreceptors with neurites extending inwards as well as outwards to the margin of the retina are visible (G). Rhodopsin labeled rod photoreceptors are visible

in the outer nuclear layer (H). VITR, vitreal (inner) aspect, SCL, sclera (outer) aspect. Scale bar = 50 microns.

Table 1

Specification of immounohistochemical markers.

Antigen	Antibody name	Target cell	Species	Dilution	Source
Neurofilament 160 KDa	Anti-neurofilament 160 clone NN18	Ganglion cells (Horizontal cells)	Mouse monoclonal	1:500	Sigma, St Louis, MO, USA
Recoverin	Anti-recoverin	Rod and cone photoreceptors	Rabbit polyclonal	1:10000	Chemicon International, Ca, USA
Vimentin	Mouse anti-vimentin	Müller cells	Mouse monoclonal	1:500	Chemicon International, Ca, USA
Rhodopsin	Rho4D2	Rod photoreceptor	Mouse monoclonal	1:100	Kind gift of Prof. RS Molday, Vancouver, Canada
Parvalbumin	Mouse anti-Parvalbumin	All amacrine cells	Mouse monoclonal	1:1000	Sigma, St Louis, MO, USA
PKC	Phospho-PKC (pan)	Rod bipolar cells (Photoreceptor outer segments)	Rabbit polyclonal	1:200	Cell Signaling, Beverly, MA, USA

Table 2

Measurements of diameters of nanofibers electrospun onto PGS membranes. ANOVA shows significant difference between all groups ($p < 0.01$).

Size (nm)	Nanofiber material			
	PCL	Laminin	Laminin-PCL	Laminin-PCL (hydrated)
Mean	175.12	65.38	101.50	199.21
Minimum	93.04	15.74	22.26	62.50
Maximum	294.22	140.81	267.41	447.43
St.Dev.	39.70	23.34	49.09	90.59

Table 3

Surgical handling results. Letter N represents no attachment. Letter A represents attachment, but insufficient for surgical application. Letter Y represents sufficient attachment for retinal transplantation.

Retina type	Membrane type				
	PGS	**RGD-PGS**	**PCL-PGS**	**Laminin-PGS**	**Laminin-PCL-PGS**
Pig (E40–50)	N	A	Y	A	Y
Pig (E99)			Y		Y